The effect of geometry dimensions on fatigue life of HFMI-treated cover plates

Citation for the original published paper (version of record):
Noghabi, M., al-Emrani, M. (2026). The effect of geometry dimensions on fatigue life of HFMI-treated cover plates. Welding in the World, Le Soudage Dans Le Monde, 70: 1637-1654. http://dx.doi.org/10.1007/s40194-025-02231-y

Welding in the World (2025) 70:1637–1654
https://doi.org/10.1007/s40194-025-02231-y

RESEARCH PAPER

The effect of geometry dimensions on fatigue life of HFMI-treated cover plates

Mohammad Noghabi[1] · **Mohammad Al-Emrani**[1]

Received: 29 July 2025 / Accepted: 26 October 2025 / Published online: 17 November 2025

Abstract
One common method to strengthen existing steel bridges is the addition of cover plates to various bridge elements. Currently, using bolted connections is preferred to welded due to the poor fatigue performance of welded connections. The use of HFMI treatment to increase the fatigue strength of welded cover plates is investigated so that welding is used instead of bolting, which will have considerable savings in terms of site work and costs. This study explores how the geometry of beams and cover plates affects the fatigue life of welded cover plates in steel bridges, particularly those treated with HFMI treatment. The effective notch stress method was employed to analyze the effects of cover plate thickness, flange thickness, and weld throat size on the stresses at the toe and root of welded cover plates. Based on the results, expressions were developed to calculate stress concentration factors at the toe and weld root for various beam and cover plate dimensions. It was found that the weld throat size plays a significant role in the stress distribution at the weld and thus on the fatigue life of welded cover plates. Furthermore, the presence of shear stress at the weld toe increases the stress concentration factor at the root, making the weld root more susceptible to root cracking. Evaluating our experimental tests and previous tests in the literature indicates that HFMI treatment significantly enhances fatigue life at the weld toe; however, if the weld root deteriorates faster than the toe, HFMI treatment becomes less effective.

Keywords Cover plate · Notch stress method · HFMI treatment · Fatigue life

1 Introduction

Many existing bridges require strengthening to accommodate the demands of heavier vehicles and increased traffic intensity, both now and in the future. Various methods can be applied to enhance the load-bearing capacity of existing bridges [1]. The addition of cover plates is a prevalent technique for reinforcing and upgrading steel bridges [2]. This method effectively raises the load-bearing capacity of structural elements by increasing their cross-sectional area and moment of inertia. Using bolted connections and welding cover plates to beams are usually utilized to connect cover plates to existing members. Bolted connection requires using fitted bolts to ensure complete load transfer between the existing member and the cover plate. Therefore, this method requires on-site drilling of both the cover plate and the strengthened component, such as a beam flange, in a single operation. In Figure 1, the beam and cover plate after hole drilling and before bolting is illustrated. While this strengthening technique is highly effective, it is also labor-intensive and costly due to the precise on-site drilling requirements [3]. Additionally, this strengthening approach has another potential drawback: the risk of crevice corrosion within the connection. This concern has been highlighted as an additional factor to consider when implementing this method. Welded cover plates are, however, vulnerable to fatigue crack growth and have lower categories in standards such as AASHTO [4] and Eurocode [5]. This situation has prompted a study into the viability of employing welded cover plates in conjunction with HFMI methods [6] to help mitigate this issue. High-frequency mechanical impact treatment (HFMI) refers to a range of high-frequency peening methods and tools, which are available under various brand names such as ultrasonic impact treatment (UIT), ultrasonic

Recommended for publication by Commission XIII - Fatigue of Welded Components and Structures

✉ Mohammad Noghabi
noghabi@chalmers.se

[1] Department of Architecture and Civil Engineering, Chalmers University of Technology, Gothenburg, Sweden

Fig. 1 An example of a beam cover plate that has been prepared for bolting onto an existing bridge girder

peening (UP), and high-frequency impact treatment (HiFIT), among others. HFMI treatment is a technique that enhances the fatigue performance of welded steel components [7]. The HFMI treatment is applied to the critical weld toes to improve the fatigue performance of structural details [8]. This method operates by reducing stress concentrations and inducing beneficial compressive residual stresses at the weld toes [9]. The process effectively counteracts or eliminates detrimental tensile residual stresses in these critical areas [9]. Additionally, HFMI treatment leads to localized cold working of the material at the weld toe, resulting in increased tensile strength in this region [7]. The fundamental principles and mechanisms underlying the HFMI method have been extensively documented in the scientific literature [8, 10].

Numerous previous studies have demonstrated that HFMI treatment is an effective technique for improving the fatigue resistance of welded connections [11–13]. Furthermore, several methods are used to estimate the fatigue life of welded details improved through HFMI treatment [14–16]. Marquis and Barsoum [10] have proposed different S-N fatigue curves for HFMI-treated welds for various steel types. The majority of fatigue tests done on HFMI-treated details were done on transversal butt welds or attachments and on longitudinal attachments. Very few tests have been reported on HFMI-treated welded cover plates.

Roy and Fisher [17] conducted experimental research on fatigue strength improvement of welded cover plates through HFMI treatment. According to their experimental results, applying HFMI treatment can enhance the fatigue resistance of cover plate connections. Their findings also indicated that this improvement becomes more pronounced when larger transverse fillet welds are used in the construction of these details. Hui et al. [18] investigated fatigue life improvement of welded cover plates subjected to 4-point bending utilizing ultrasonic impact treatment. In their study of the twenty cover plate ends that underwent HFMI treatment, twelve experienced failures originating from the weld root, while only three ends developed cracks starting at the weld toe. Consequently, these test results suggest that designers should carefully consider the possibility of root cracking when employing HFMI-treated welded cover plates. Leitner and Stoschka [19] conducted an experimental investigation to evaluate the IIW-recommended fatigue assessment procedures for HFMI-treated high-strength steel cover plates under various stress ratios. The loading condition was tension loading in their study. They found that the effective notch stress approach may underestimate fatigue damage at higher stress ratios ($R = 0.5$). Therefore, they suggested a more pronounced reduction in the FAT-class for high R-ratios to ensure conservative design. Vilhauer et al. [20] examined the potential synergies between various repair techniques applied to welded cover plates subjected to 3-point bending. Fifteen fatigue tests were carried out in their study, revealing that ultrasonic impact treatment significantly enhanced the fatigue life of cover plate end details. This significant improvement effectively elevated the fatigue performance of these details from an AASHTO fatigue Category E classification (corresponding to Eurocode detail category 56) to that of an AASHTO fatigue Category A (corresponding to Eurocode detail category 160), standing for a substantial enhancement in durability and structural integrity. Al-Emrani et al. [3] conducted both experimental and numerical studies to investigate the fatigue life improvement of beams strengthened with cover plates welded in the middle of the beam using HFMI treatment. Their experimental results showed that HFMI treatment enhances the fatigue strength of welded cover plates by more than four detail categories.

Excluding the tests reported by Leitner and Stoschka [19] and Vilhauer [20], which were conducted on simple plates strengthened with welded cover plates, there still exist very few tests that can be used to verify the fatigue life improvement that can be achieved by HFMI treatment of welded cover plates. Furthermore, some tests report failure originating from the weld root, which might put an upper limit on what fatigue strength improvement can be accounted for from HFMI treatment of these details. This gap in research shows a need for further comprehensive investigations into the specific conditions that influence the fatigue strength of HFMI-treated cover plates and particularly those leading to toe cracking or root cracking being the governing cracking mode. Additionally, factors

Table 1 The chemical composition of S355 steel

C	Si	Mn	P	S
0.23	0.05	1.6	0.05	0.05

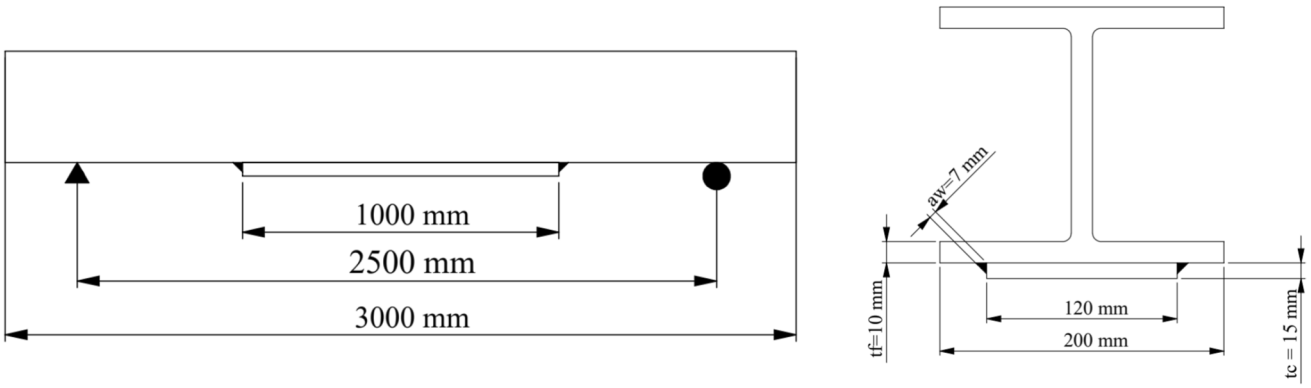

Fig. 2 The configuration and dimensions in the experimental tests

Table 2 The geometry dimensions of experimental tests

Beam Type	No. of tests	t_f	t_c	a_w	Treatment
HEA 200	8	10	15	7	HFMI
HEA 200	4	10	15	7	As welded

such as cover plate thickness, beam flange thickness, and weld throat size should be examined further. Designers also need reliable models to estimate the fatigue strength of HFMI-treated cover plates without the need for complex finite element analyses.

2 Method

2.1 Experimental tests

The experimental tests were done on welded cover plates made of S355 steel. The chemical composition of S355 is presented in Table 1.

HEA 200 beams were used in the experimental tests. The configuration and dimensions are illustrated in Figure 2. The cover plate was welded to beam with spray arc using ESAB Autrod 12.51 1.2-mm solid wire. The experimental tests are summarized in Table 2.

Eight specimens were HFMI treated by HiFit HFM21R1 machine at a controlled speed using a 3-mm pin diameter. The process was performed manually in a single pass. It started 200 mm from the cover plate corner in the longitudinal weld and applied continuously around the cover plate end, ending 200 mm from the other corner. The HFMI treatment speed was 5–30 mm/s. The average speed was about 15 mm/s; the treatment speed changed only in the corners of cover plate. Figure 3 shows the specimen after HFMI treatment. The groove dimensions were measured using 3D scanning. The average groove depth is about 0.15 mm, and the average diameter is about 3.2 mm. It should be noted that the groove diameter is a little larger than the pin diameter due to aberration and lateral movement of the pin [21]. Four specimens were tested without any treatment (as-welded condition).

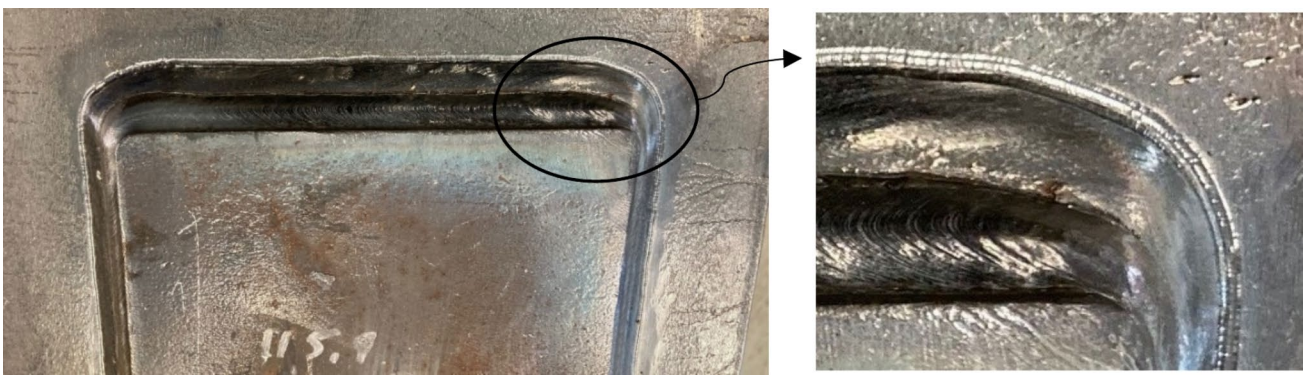

Fig. 3 The HFMI-treated specimen [3]

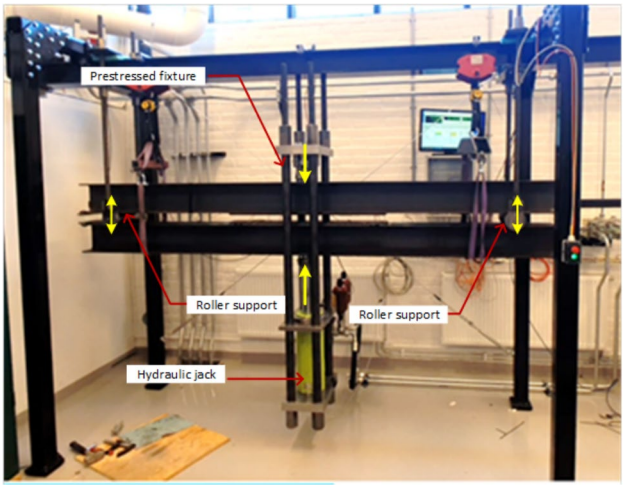

Fig. 4 The set-up for fatigue testing of beams

Table 3 The geometry dimensions of experimental tests in literature

Reference	t_f	t_c	a_w	Treatment
Vilhauer et al. [20]	25.4	25.4	7.94	HFMI
Hui et al. [18]	28	25.4	9	HFMI

The fatigue tests were conducted using a dedicated fatigue testing machine designed for evaluating beams under bending loads which allows for testing 2 beams simultaneously. The hydraulic jack introduces force to the bottom beam, and due to roller supports and prestressed fixture, the same loading is transferred to top beam. When the crack occurred in one of the specimens, the test was stopped, and the cracked specimen was replaced with a dummy beam and then the test continued to failure of the second beam. Constant amplitude loading (CAL) tests were conducted with an R-ratio of 0.1, and the loading frequency was 7 Hz. To facilitate early crack detection, all test specimens were instrumented with strain gauges. The fatigue loading stopped when the crack propagated through the flange thickness, which is considered as failure. The crack growth was not measured during fatigue loading. The experimental setup for applying cyclic loading to the specimens is illustrated in Figure 4.

Furthermore, the experimental test available in the literature ([20] and [18]) were also analyzed to cover different thicknesses and weld throat sizes (see Table 3).

2.2 Finite element modelling

The numerical investigation employed in the current study deals with S355 structural steel beams with welded cover plates. The dimensions of the beams and cover plates are illustrated in Fig. 5, in which L_b represents the beam length, L_c is the cover plate length, H_b is the beam height, H_w is the web height, W_c is the cover plate width, W_b is the beam flange width, t_c is the cover plate thickness, t_f is the beam thickness, and a_w is the weld throat size.

The effective notch stress (ENS) method is used to assess the local stresses at the weld toe and root sides of the cover plate. To compute these stresses, numerical methods such as the finite element method (FEM) or the boundary element method (BEM) are utilized.

The FE analysis was performed using the software Abaqus/CAE. Since the specimen exhibits symmetric geometry and loading, only one-quarter of the specimen is modelled. An efficient meshing approach is discussed by Baumgartner et al. [22]. In their study, the required mesh in the notch zone, which is appropriate for the notch stress method, is investigated. They provided some recommendations to create appropriate mesh for different element types. The mesh at the root and toe areas must be sufficiently refined. The IIW recommendation for element size is provided in Table 4. Mesh sensitivity analysis was performed to ensure that the mesh size is appropriate (Fig. 6). Figure 6 shows the convergence of the stress concentration factor at the weld root, K_{root}, for different element sizes. The mesh configuration used in the finite element model is illustrated in Fig. 7.

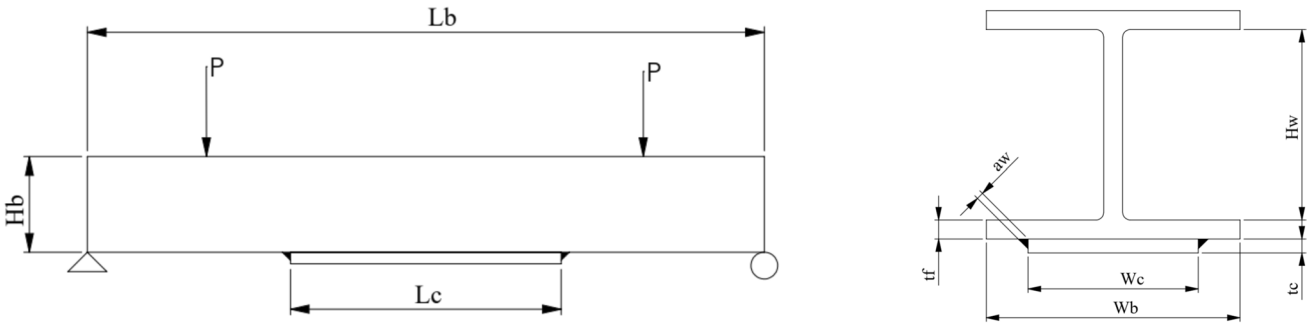

Fig. 5 The dimensions of the beam and cover plate

Table 4 IIW recommendation for meshing according to ENS

Element type	Relative size	$r_{ref} = 1$ mm	$r_{ref} = 0.05$ mm
Quadratic	$\leq \frac{r}{4}$	$\leq 0.25\ mm$	$\leq 0.012\ mm$
Linear	$\leq \frac{r}{6}$	$\leq 0.15\ mm$	$\leq 0.008\ mm$

C3D8R (eight-node brick with reduced integration) elements are used near the toe and the root regions in these analyses.

The ENS was performed on 122 models with different geometrical properties. For each case, the load applied to the beam was determined so that the nominal stress at the weld toe is 1 MPa. Thus, the stresses at the toe and root notches are equal to stress concentration factors at these two locations ($\sigma_{toe} = K_{toe}$ and $\sigma_{root} = K_{root}$). Therefore, in the following, reference will always be made to these stress concentration factors, i.e., K_{toe} and K_{root}. In Fig. 8, the effective notch stress (maximum principal) is illustrated. The fatigue crack tends to grow in the perpendicular direction to the maximum stress.

The root can be modelled as a keyhole shape or fillet-type [23]. In our analysis, the root is modelled as a keyhole shape, and it is tangential to the root location (Figure 9).

2.3 Selection of parameters for parametric study

The numerical study comprised a total of 122 beams with various flanges, cover plates, and weld throat thicknesses. These values were chosen to cover what is typical for the application of cover plates in bridges. The analyses were done for different beam and cover plate dimensions and for different weld sizes. The analyses are presented in Table 5.

3 Results

In the following, the results from the numerical study are analyzed to identify the most influential geometric parameters on the stress concentration at the weld toe and root sides. The experimental results are also provided and discussed.

3.1 The effect of loading conditions

The effect of loading conditions was evaluated for four different cases, including pure bending (4-point bending where the cover plate is between loading points (Fig. 5)), tension loading, uniformly distributed loading, and a concentrated force at midspan of the beam (3-point bending). The beam length is 6 m, and the cover plate length is 2.4 m. The stress concentration factors at the toe and root for $t_c = 20$, $t_f = 30$, and a_w/t_c are presented in Table 6 for these four different loading conditions. As can be seen, the root and toe stress concentration factors for pure bending and tension loading

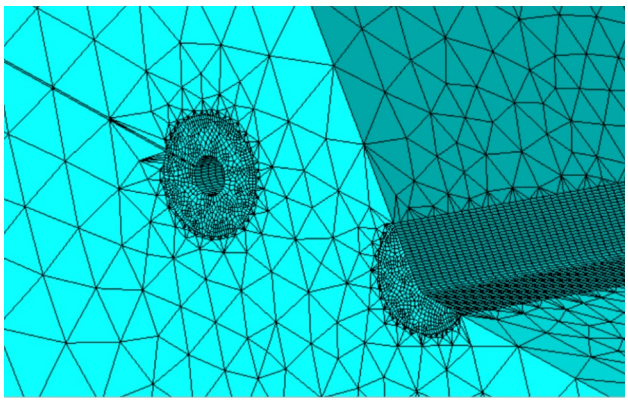

Fig. 7 The applied mesh in FEM

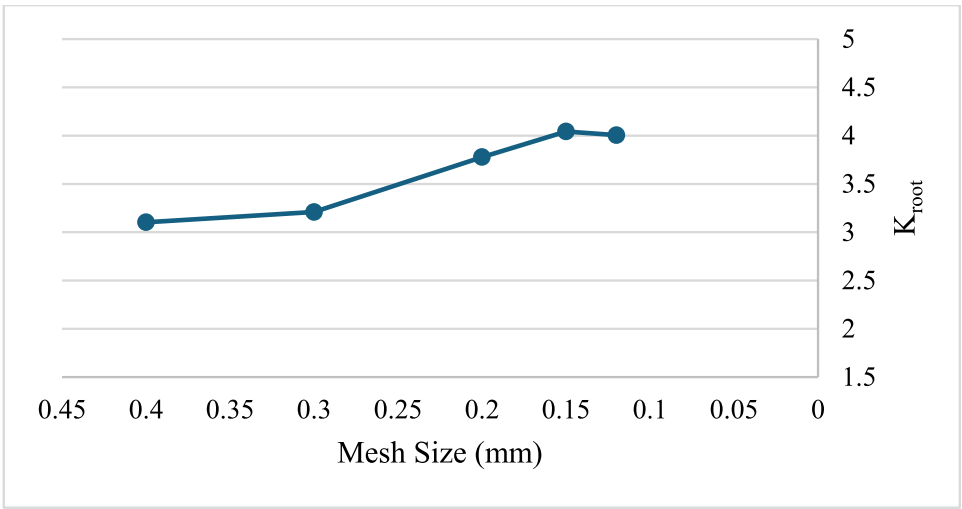

Fig. 6 The mesh sensitivity analysis

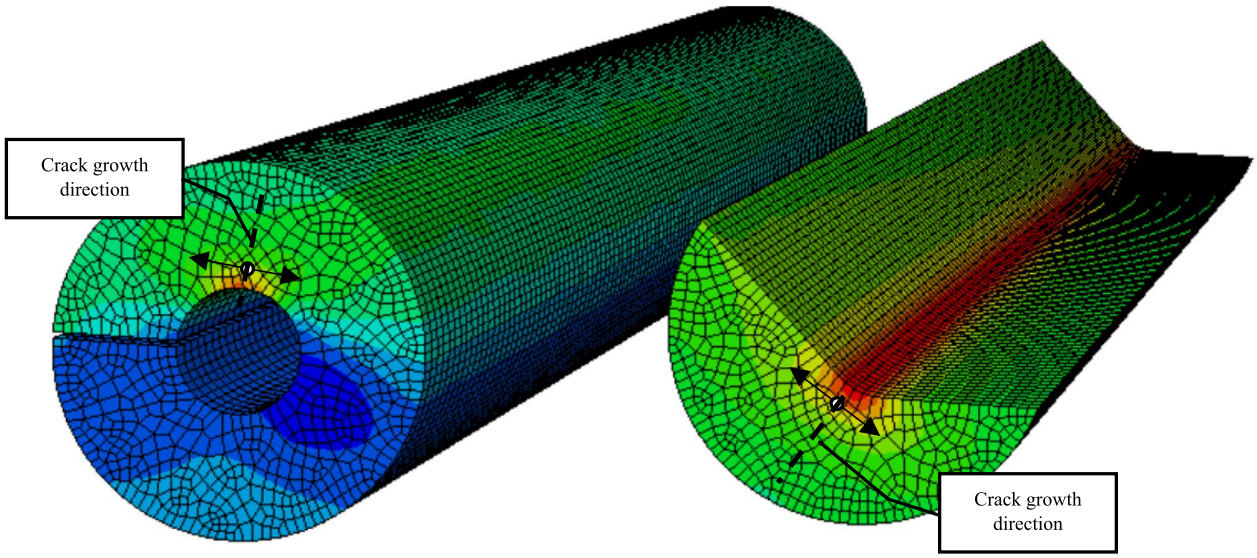

Fig. 8 The effective notch stress (maximum principal) in the weld toe and root

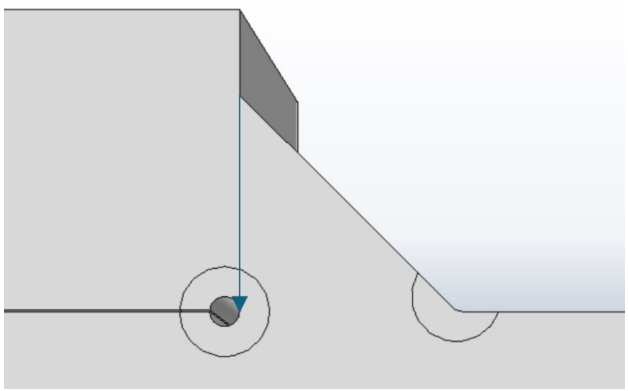

Fig. 9 Keyhole shape at the root location

Table 5 Different parameters and dimensions in analyses

t_f	t_c/t_f	a_w/t_c
15	0.66, 0.8, 1, 1.66, 2	0.25 to 0.7
20	0.5, 0.6, 0.75, 1, 1.5	0.25 to 0.7
30	0.4, 0.5, 0.66, 0.83, 1, 1.33	0.25 to 0.7
40	0.3, 0.5, 0.75, 1	0.25 to 0.7
50	0.24, 0.4, 0.6	0.25 to 0.5

(which have no shear stress) are less than other loading situations. The stress ratio, K_{toe}/K_{root}, is, however, bigger for pure bending and tension loading. The 3-point loading scheme provides the worst case (in terms of generating the highest stress concentration factors). This is reflected by the fact that this loading condition produces higher stress concentration

Table 6 Stress concentration factors at weld toe and root for different loading conditions

	τ/σ	K_{toe}	K_{root}	K_{toe}/K_{root}
Pure bending	0	5.481	4.043	1.356
Tension loading	0	5.042	3.813	1.322
Uniformly distributed load	0.117	5.617	4.401	1.276
3-point bending	0.205	5.866	4.838	1.212

Table 7 The impact of the existence of shear stress

	K_{toe}	K_{root}	K_{toe}/K_{root}
Shear Stress	6.615	5.474	1.208
No Shear Stress	5.481	4.043	1.356

at both toe and root and also the lowest K_{toe}/K_{root} ratio which indicates higher risk for root cracking. Since shear stress has a major impact on stress concentration factors, the pure bending condition was used in our simulations to neglect the effect of shear stress.

3.2 The effect of the existence of shear stress

The impact of the presence of shear stress at the weld toe on the stress concentration at the toe and root was analyzed by extending the cover plate to be terminated in the shear region (in the 4-point bending case with the load still being applied to obtain 1 MPa nominal stress at the end of the cover plate). The stress concentration factor at the weld toe and root is illustrated in Table 7. As can be seen, stress concentration

factors increase when there is shear force to be transferred to the cover plate. In addition, the ratio K_{toe}/K_{root} is reduced when the cover plate is terminated in the shear region. This is because the increase in K_{root} is more than the increase in K_{toe}. Decreasing the K_{toe}/K_{root} increases the possibility of root cracking.

3.3 The effect of cover plate length

A set of analyses were done for three different cover lengths to investigate the effect of cover plate length. The loading condition is uniformly distributed loading, so the studied cases would be indicative of the ratio of shear to bending stresses at the cover plate end. In Figure 10, the effect of cover plate length on the stresses at the weld toe and root is illustrated. As can be seen, increasing the cover plate length leads to an increase in the stresses at the weld toe and root. The stress ratio is, however, not changed.

3.4 The effect of flange thickness

The impact of flange thickness on the fatigue performance of welded cover plates was analyzed. In this study, various flange thicknesses (20, 30, 40, and 50 mm) were examined while keeping all other dimensions unchanged ($t_c = 20mm$, $a_w/t_c = 0.5$). The K_{toe}, K_{root}, and the ratio of K_{toe} to K_{root}, K_{toe}/K_{root}, for different values of flange thickness are shown in Fig. 11. As can be seen, the change in flange thickness results only in a minor change in stress concentration factor at toe, root, and the ratio K_{toe}/K_{root}.

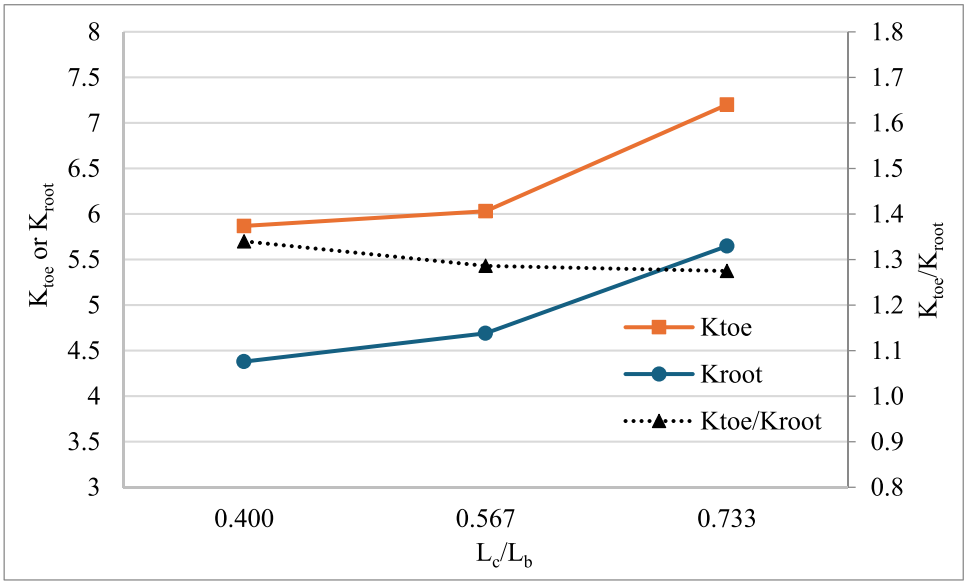

Fig. 10 The effect of the cover plate length on the K_{toe}, K_{root}, and the ratio

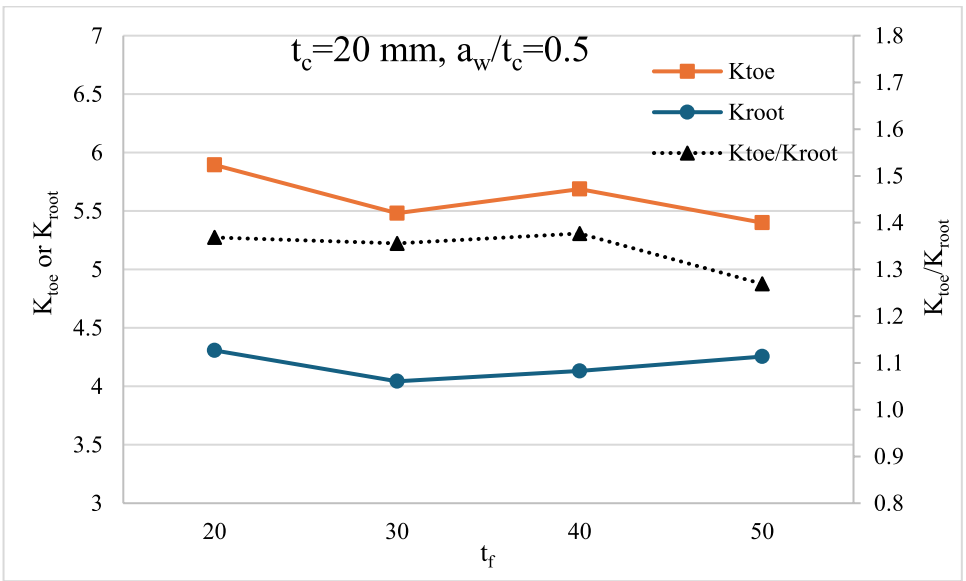

Fig. 11 K_{toe},K_{root}, and the ratio of K_{toe} to K_{root} versus the flange thickness (t_f)

3.5 The effect of weld throat size

The influence of weld throat size (a_w) on stresses at the weld toe and root was examined. In this study, only the weld throat size was varied while all other dimensions remained unchanged. Three different weld throat sizes to cover plate thickness ratios are considered (0.25, 0.35, and 0.5). The FE analyses were done for two different flange thicknesses. The stress concentration factors at the toe, root, and their ratio, K_{toe}/K_{root}, for different values of a_w/t_c are shown in Fig. 12. As can be seen, the change of the weld size results in a major change in stress concentration factors at the weld toe and root. Increasing the weld throat size results in a reduction in stress concentration factors. The rate of reduction in the root being larger than it is in the toe. So, decreasing the weld throat size leads to a reduction in K_{toe}/K_{root}.

3.6 The effect of cover plate thickness

As the stress concentration at weld toe and root was found to be highly influenced by the ratio a_w/t_c, the variation of K_{toe} and K_{root} as a function of the ratio of cover plate thickness to flange thickness (t_c/t_f) was studied for different a_w/t_c, which is illustrated in Figs. 13 and 14. As observed, the stress concentration factors at the root do not show any significant correlation with t_c/t_f (it is however highly dependent on a_w/t_c). It seems that the stress concentration factors at the toe are, on the other hand, slightly influenced by the ratio t_c/t_f specially for smaller values of a_w/t_c. The stress concentration factors at toe and root are greater for smaller values of a_w/t_c.

Consequently, K_{toe}/K_{root} becomes also dependent on the ratio t_c/t_f particularly for smaller values of a_w/t_c (Fig. 15).

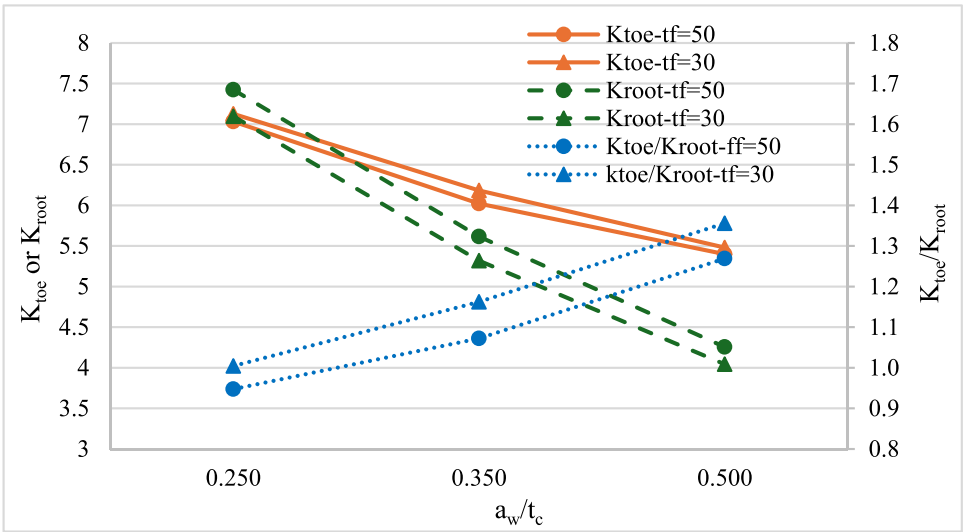

Fig. 12 K_{toe}, K_{root}, and the ratio of K_{toe} to K_{root} versus the weld throat size to cover plate thickness ratio

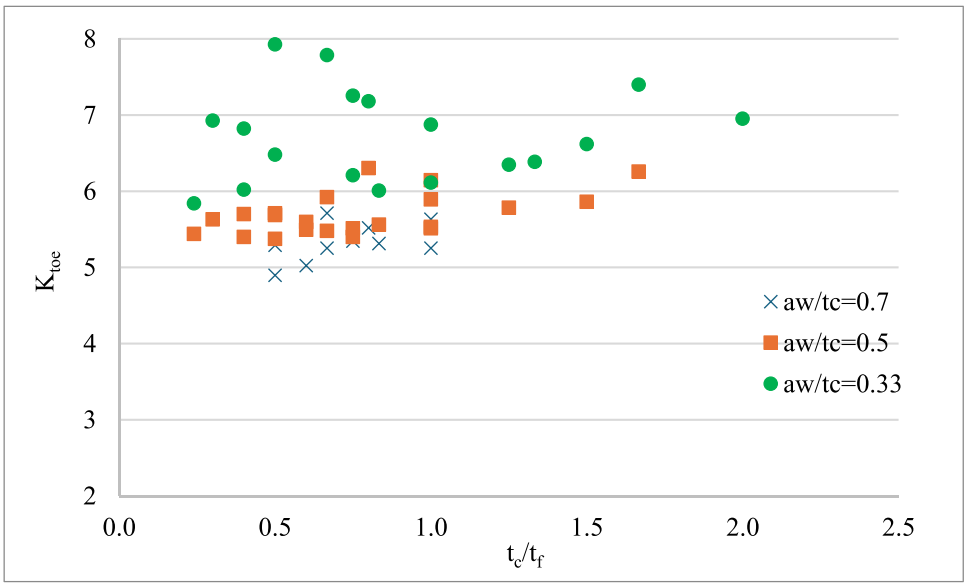

Fig. 13 Variation of K_{toe} as a function of t_c/t_f for different a_w/t_c

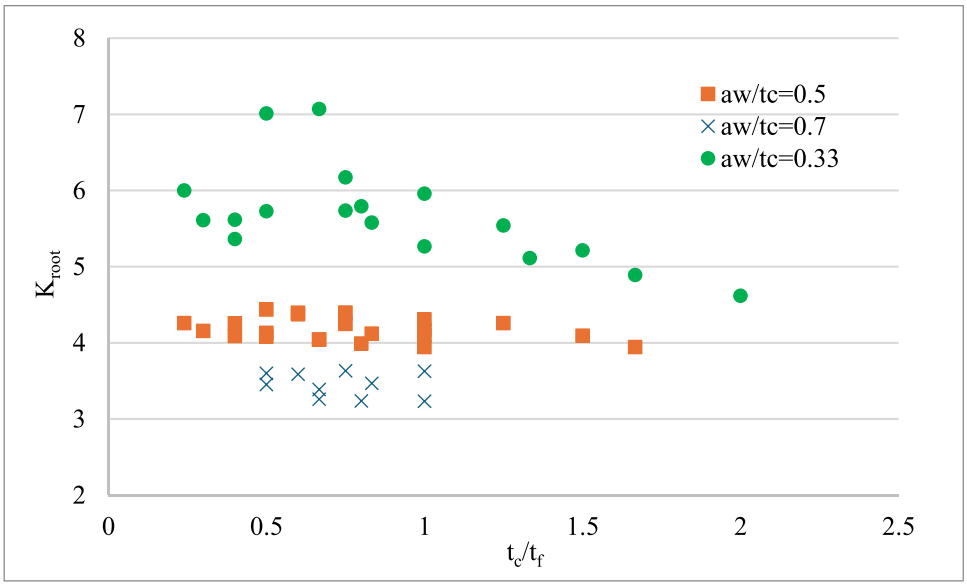

Fig. 14 Variation of K_{root} as a function of t_c/t_f for different a_w/t_c

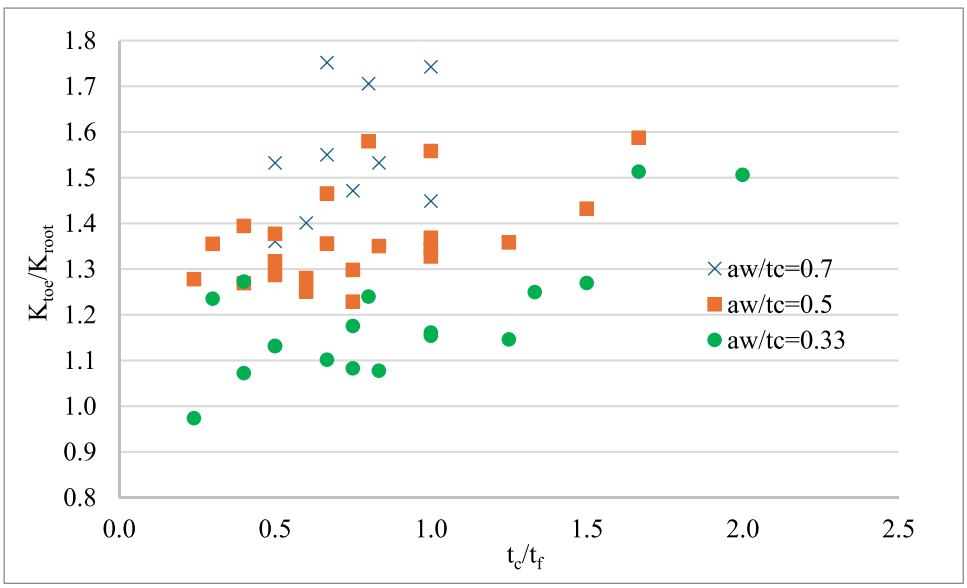

Fig. 15 The ratio of K_{toe} to K_{root} versus the cover plate thickness (t_c/t_f) for different a_w/t_c

The K_{toe} and K_{root} as a function of the ratio of cover plate thickness to flange thickness for $a_w/t_c = 0.5$ for various flange thicknesses is illustrated in Figs. 16 and 17. The stress concentration factor at toe, K_{toe}, for the 15 mm flange thickness is greater than other flange thicknesses. The stress concentration factor at root, K_{root}, for the 15 mm flange thickness is less than other flange thicknesses.

The ratio, K_{toe}/K_{root}, for different t_c/t_f and $a_w/t_c = 0.7$ is shown in Fig. 18. This ratio is bigger for 15 mm flange thickness than other thicknesses but otherwise is insensitive to t_c/t_f.

3.7 Experimental results

Fatigue testing was stopped when the crack had propagated through the beam flange thickness. The failure mode of both as-welded and HFMI-treated specimens was toe-cracking (see Figure 19). The fatigue test results are summarized in Table 8.

The fatigue test results for both as-welded and HFMI-treated samples are plotted in Figure20. For the HFMI-treated results, statistical evaluation was made enforcing

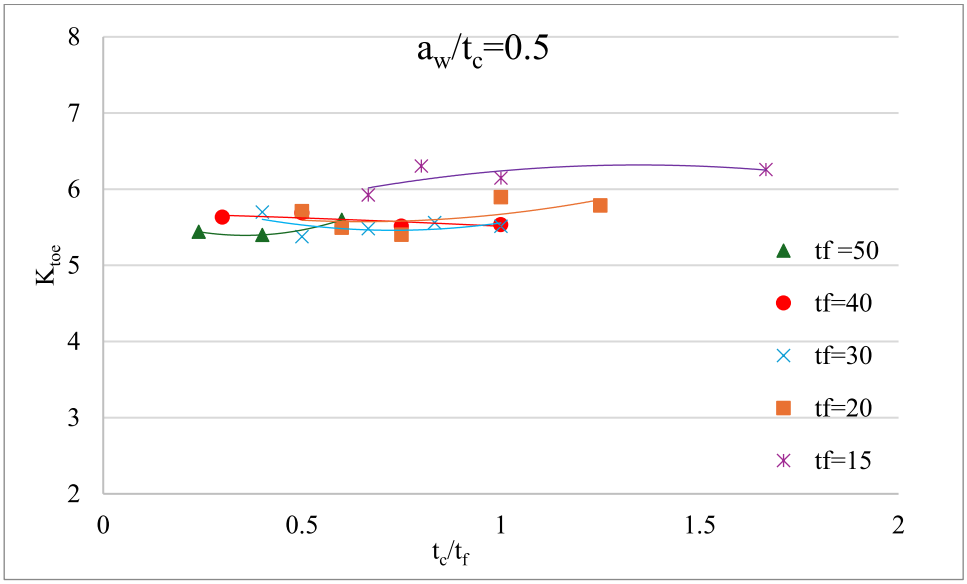

Fig. 16 Variation of K_{toe} as a function of t_c/t_f for $a_w/t_c = 0.5$

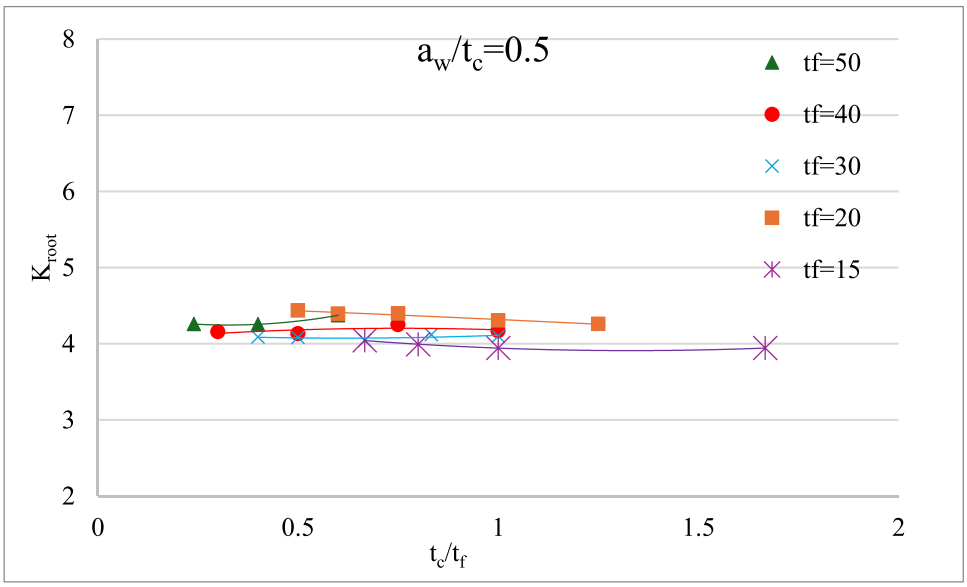

Fig. 17 Variation of K_{root} as a function of t_c/t_f for $a_w/t_c = 0.5$

a slope of 5; a detail category (95% fractile) of 81.4 MPa is obtained with a standard deviation of 0.174. The closest detail category in EN 1993-1−9 is 80 MPa. The number of tests conducted in the as-welded condition is too small to support a valid statistical assessment of the detail category. These tests are presented with reference to detail category 50, deemed suitable in accordance with EN 1993-1−9. The findings indicate that HFMI treatment led to a fatigue strength improvement equivalent to four detail categories. This is one category lower than the enhancement recommended by the IIW for steels with yield strengths ranging from 355 to 550 MPa [3].

4 Stress concentration factors with respect to weld toe and root

The results of the 122 beams analyzed are used to fit expressions for estimating the stress concentration factors at the weld toe and root as well as the ratio of stress

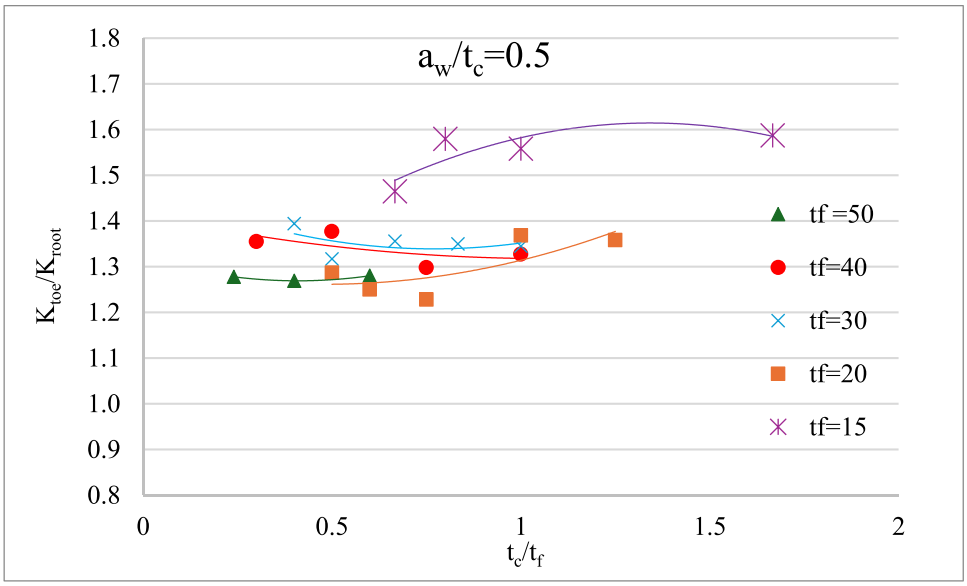

Fig. 18 The ratio of K_{toe} to K_{root} versus t_c/t_f for $a_w/t_c = 0.5$

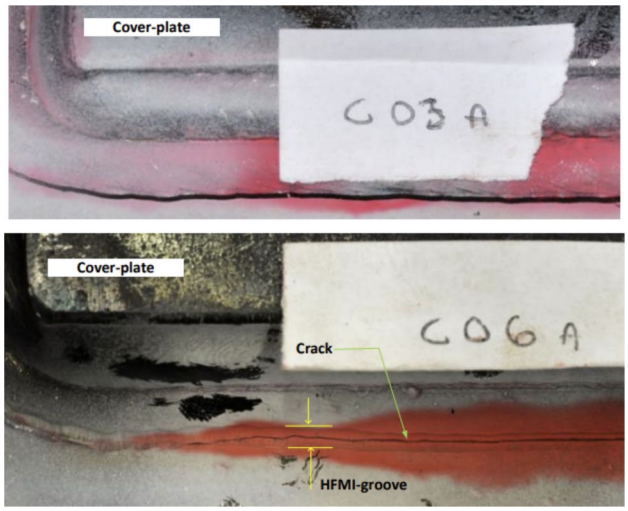

Fig. 19 Fatigue cracks in the as-welded (C03) and HFMI-treated (C06) specimens [3]

Table 8 Fatigue test results [3]

Beam No	*Type*	*Δσ (MPa)*	$N_{failure}$ (×1000)
C01	As-welded	67.5	1299
C02	As-welded	67.5	1139
C03	As-welded	67.5	1320
C04	As-welded	67.5	1490
C05	HFMI	96.4	3054
C06-1	HFMI	96.4	Run-out
C06-2	HFMI	115.4	1685
C07	HFMI	115.4	759
C08	HFMI	115.4	541
C09	HFMI	105.8	950
C10	HFMI	105.8	1850
C11	HFMI	105.8	1480
C12	HFMI	105.8	1001

concentration factors. These expressions would be needed to perform fatigue design of HFMI-treated welded cover plates without the need for detailed ENS analysis of the strengthened structure-member.

The stress concentration factors for different geometrical parameters such as weld throat thickness (a_w), cover plate thickness (t_c), flange thickness (t_f), moment of inertia of Beam and cover plate (I_b and I_c), the width of cover plate and beam flange (W_c and W_b), and area of cover plate and beam (A_c and A_b) are determined using ENS finite element analysis. Since stress concentration factors are unitless, the effective parameters analyzed as the ratio to have a unitless expression. Curve fitting was conducted using genetic algorithms optimization in MATLAB [24] recognizing that the geometrical properties that have the most influence on the stress at the weld toe and root are weld throat thickness in addition to flange and cover plate thickness, expressed in ratios, i.e., a_w/t_c and t_c/t_f. Other presumably influencing ratios, such as the ratio of moment of inertia and area of the cover plate to that of the beam (I_c/I_b and A_c/A_b), were also examined but were found to have very small and ambiguous influence and were therefore disregarded. Various combinations of parameters such as the power equation and multiplication of factors were examined to find the best expression to estimate stress concentration factors. Different expressions were derived and compared with each other. The difference between our simple expressions and other more comprehensive formulas was negligible. Furthermore, a machine learning algorithm was developed to find a better solution. The

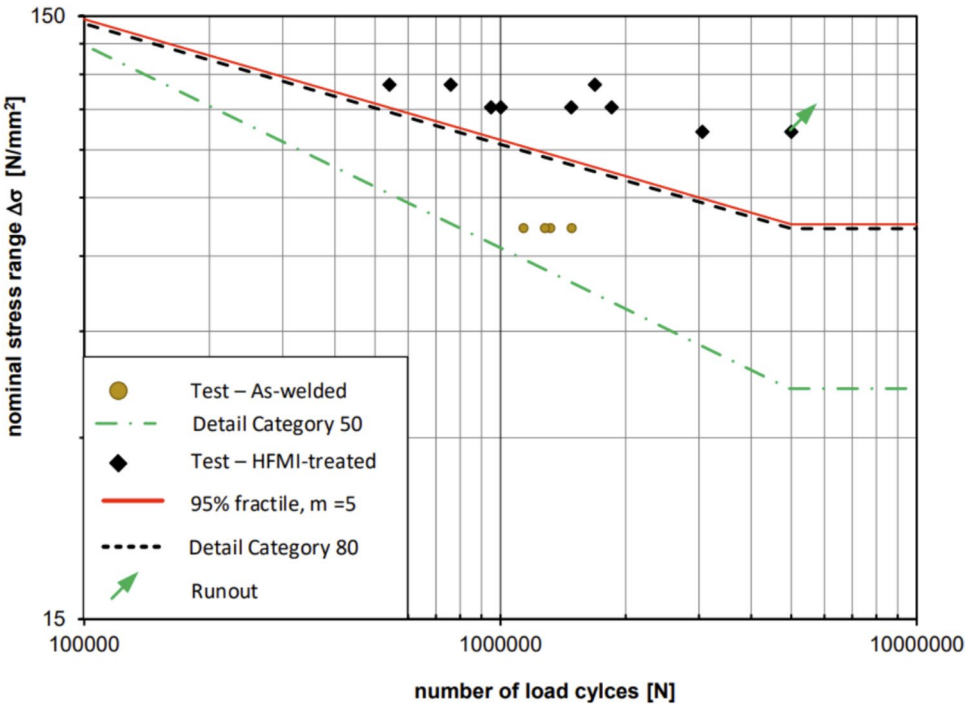

Fig. 20 Fatigue test results for the as-welded and HFMI-treated specimens [3]

Table 9 Coefficient of A and B

t_f	A	B
15	$5\times\left(\frac{t_c}{t_f}\right)^{0.11}$	$-0.25\times\left(\frac{t_c}{t_f}\right)^2+0.25\times\left(\frac{t_c}{t_f}\right)-0.776$
20	$4.65\times\left(\frac{t_c}{t_f}\right)^{0.21}$	$-0.4\times\left(\frac{t_c}{t_f}\right)^2+1.15\times\left(\frac{t_c}{t_f}\right)-1.04$
30–50	4.67	−0.26

accuracy of that algorithm is better, but it was much more complicated, so it was neglected. In the following, the last simple formulation that gave the best fit to FE results is presented.

An expression for estimating the root stress concentration factor, K_{root}, with $R^2=0.927$ (Fig. 21) is derived as follows:

$$K_{root}=2.4\left(\frac{a_w}{t_c}\right)^A \tag{1}$$

where $A = 0.119\left(\frac{t_c}{t_f}\right)-0.855$

This formula is in good agreement with the results obtained in the previous section. The stress concentration factor at the root mainly depends on the a_w/t_c.

The stress concentration factor at toe, K_{toe}, is as follows:

$$K_{toe}=A\left(\frac{a_w}{t_c}\right)^B \tag{2}$$

The A and B coefficients are found to be different depending on flange thickness and can be expressed in terms of the ratio t_c/t_f, with the values given in Table 9.

These formulas are in good agreement with the results obtained in the previous section. The stress concentration factor at the toe mainly depends on the a_w/t_c but also on the t_c/t_f. Furthermore, it is different for various flange thicknesses especially for thinner flanges.

In Fig. 21, the regression plot of predicted data versus the actual data for K_{toe} is plotted.

The derived expression for estimating stress ratio with $R^2 = 0.82$ (Figure 22) is as follows:

$$\frac{K_{toe}}{K_{root}}=1.84\left(\frac{a_w}{t_c}\right)^{0.5}+0.057\left(\frac{t_c}{t_f}\right)^3 \tag{3}$$

This formula is in good agreement with the results obtained in the previous section. The stress concentration ratio mainly depends on the a_w/t_c. It shows a minor relevance to t_c/t_f.

In order to more clearly demonstrate the influence of various geometric entities on the stress concentration factors and their ratio, the derived expressions for K_{toe}, K_{root}, and K_{toe}/K_{root} are used in the following.

The stress concentration factor at the weld toe, K_{toe}, for various flange thicknesses for $t_c/t_f = 0.75$ is plotted in Fig. 23. It is illustrated that K_{toe} decreases when weld throat size increases. K_{toe} is greater for smaller flange thickness. This result is in agreement with results obtained in previous section (Figs. 13 and 16).

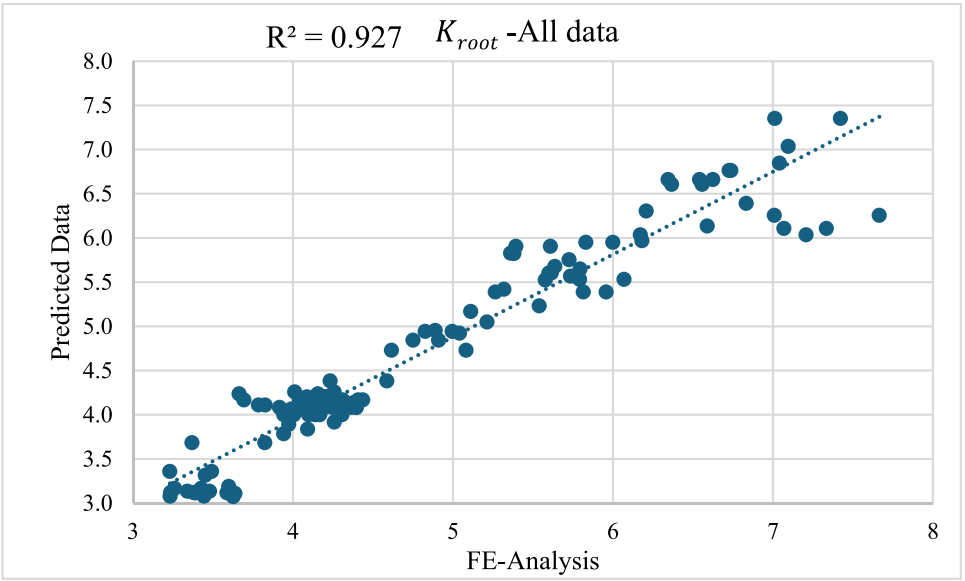

Fig. 21 The predicted data versus the FE-analysis data for K_{root}

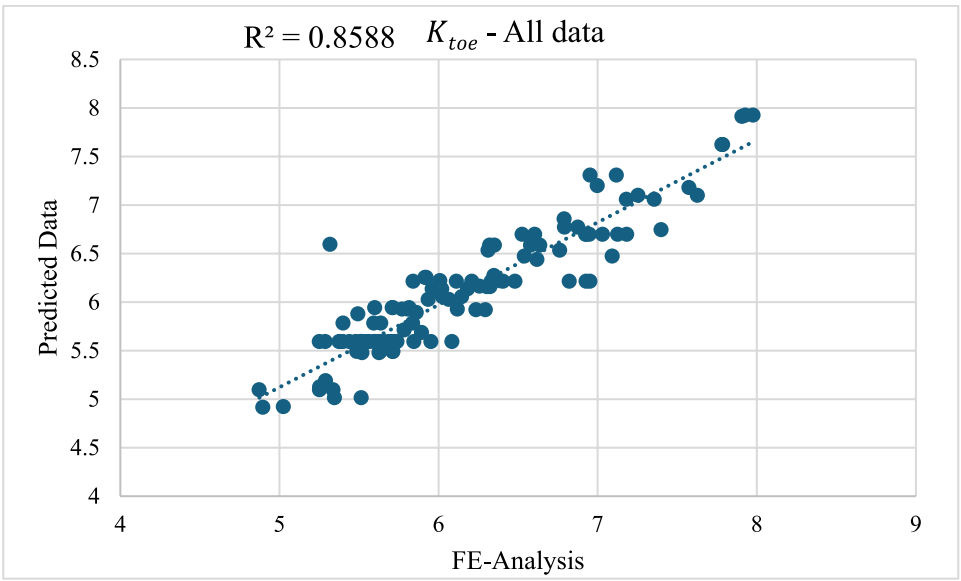

Fig. 22 The predicted data versus the FE-analysis data for K_{toe}

The stress concentration factor at the weld toe, K_{toe}, for flange thicknesses of 15 and 20 mm is plotted in Figs. 24 and 25. As can be seen, the slope of the curve is greater for smaller values of t_c/t_f. This indicates that when the thickness of the cover plate is smaller than the flange thickness, K_{toe} is more sensitive to weld throat size, or—in other words—larger t_c/t_f requires smaller a_w/t_c to produce the same stress concentration factor at the weld toe.

The stress concentration factor at the weld root, K_{root}, for flange thickness in the range of 15 to 50 mm is plotted in Fig. 26. As can be seen, the stress concentration factor at the weld root is strongly dependent on a_w/t_c and t_c/t_f has only a minor effect for smaller a_w/t_c values (below 0.5). This result is in agreement with Figs. 14 and 17.

In Fig. 27, the ratio of K_{toe}/K_{root} is plotted as a function of a_w/t_c for different values of t_c/t_f. It can be seen that t_c/t_f has a moderate effect on the stress concentration ratio, which increases slightly when this ratio increases, but that this ratio is primarily influenced by a_w/t_c.

5 Estimation of cracking mode and fatigue life of HFMI-treated cover plates

The fatigue life of the welded cover plate details can be calculated based on Eqs. (4) and (5) with respect to root and toe, respectively. In these formulas, $\alpha = \Delta\sigma_{toe}/\Delta\sigma_{root}$ is the stress ratio, $\Delta\sigma_{c\_root}$ is the detail category for root

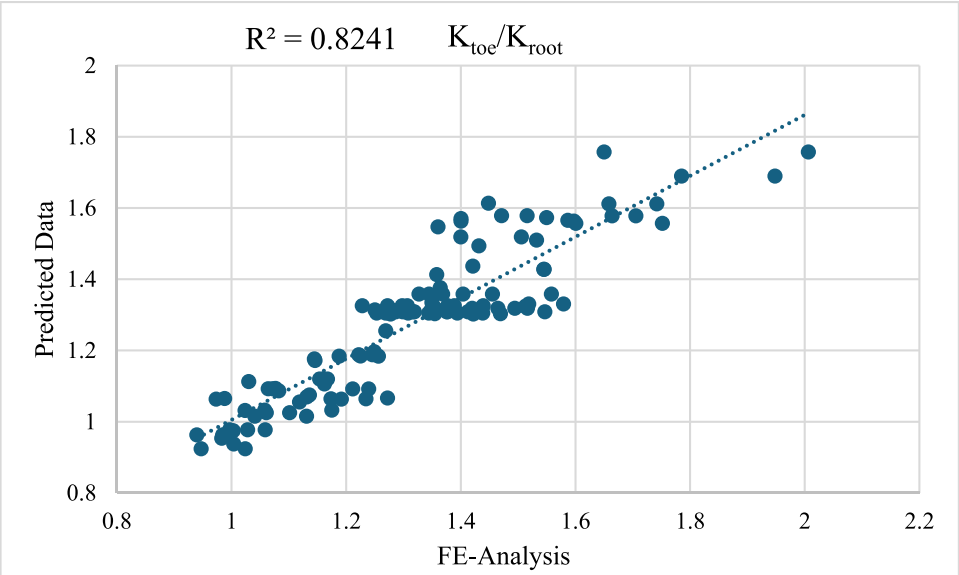

Fig. 23 The predicted data versus the FE-analysis data for K_{toe}/K_{root}

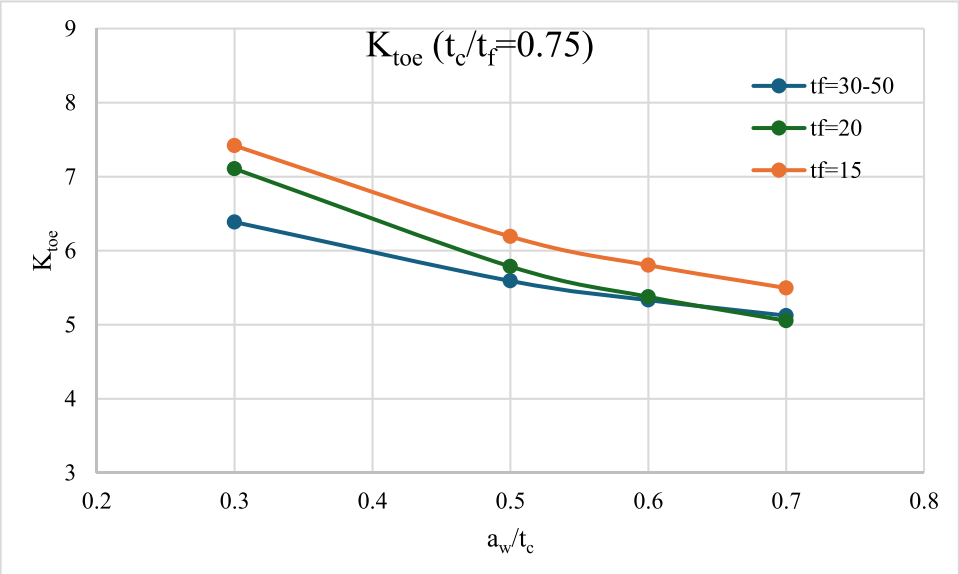

Fig. 24 The K_{toe} versus the weld size to cover plate thickness ratio for $t_c/t_f = 0.75$

cracking (225 MPa), and $\Delta\sigma_{c\_toe}$ is the detail category for HFMI-treated (320, 360, etc., based on the yield stress), both in the effective notch stress system. Constant amplitude loading (CLA) and $R < 0.15$ are assumed. Higher R ratio would result in FAT reduction. This study is concerned with welded cover plates on existing structures. Previous studies on bridge loading have shown that the influence of varying R-ratios from traffic loads on road bridges is very limited [25, 26]. Therefore, the results presented are valid for application on existing structures.

$$N_{root} = 2 \times 10^6 \left(\frac{\Delta\sigma_{c\_root}}{\frac{1}{\alpha}\Delta\sigma_{toe}} \right)^3 \tag{4}$$

$$N_{toe} = 2 \times 10^6 \left(\frac{\Delta\sigma_{c\_toe}}{\Delta\sigma_{toe}} \right)^5 \tag{5}$$

For different values of α, the stress at which the cracking mode changes from toe to root cracking can be expressed as follows:

$$\Delta\sigma^*_{toe} = \frac{\sqrt{\alpha^3 \Delta\sigma_{c\_root}{}^3 \Delta\sigma_{c\_toe}{}^5}}{\alpha^3 \Delta\sigma_{c\_root}{}^3} \tag{6}$$

As seen, $\Delta\sigma^*_{toe}$ depends on the detail category for toe and root cracking as well as on the ratio of stress concentration factors, $\alpha = \Delta\sigma_{toe}/\Delta\sigma_{root}$. This is illustrated in Fig. 28,

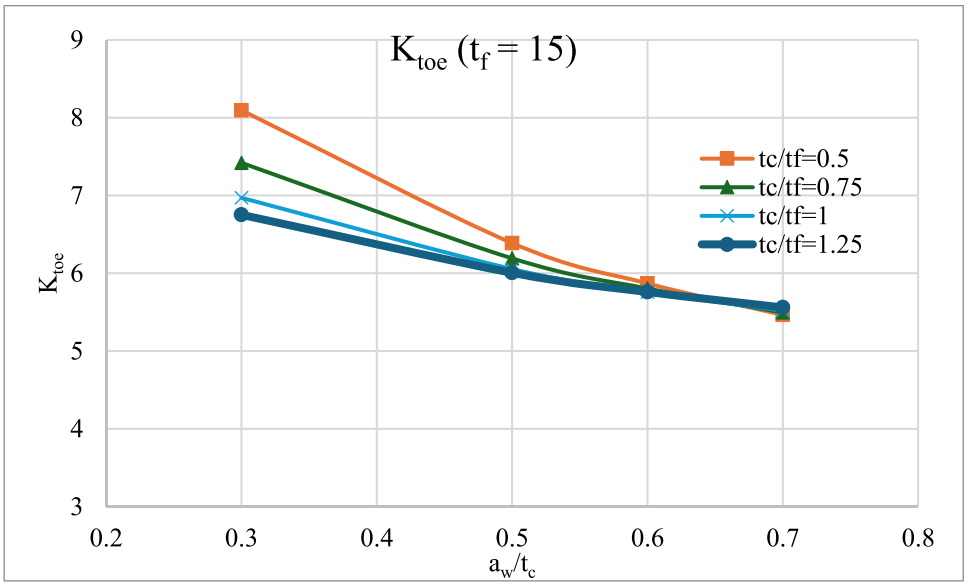

Fig. 25 The K_{toe} versus the weld size to cover plate thickness ratio for t_f = 15

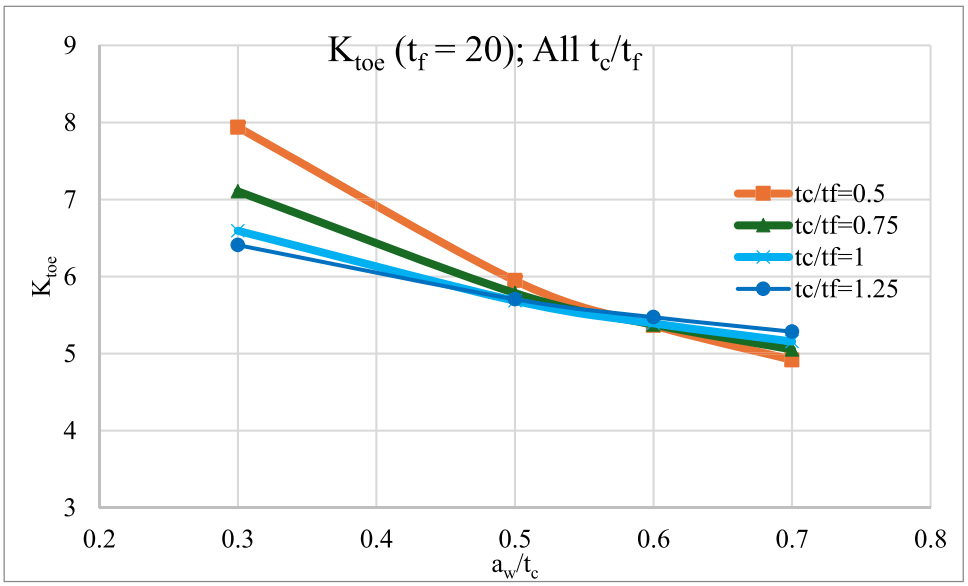

Fig. 26 The K_{toe} versus the weld size to cover plate thickness ratio for t_f = 20

where the S–N curves for different values of α are plotted. The governing cracking mode will change from toe to root cracking at different stress ranges, dependent on the value of α.

Using Eq. (6), one can construct a toe-to-root failure chart, for a given $\Delta\sigma_{c\_toe}$ ($\Delta\sigma_{c\_root}$ being 225 MPa always). This is done in Fig. 29 for $\Delta\sigma_{c\_toe} = 360MPa$ (corresponding to HFMI-treated welds in steel S355 according to IIW recommendation). The curve shows the relation of $\Delta\sigma_{toe}$ vs. $\Delta\sigma_{root}$ in log–log scale at which fatigue cracking will turn from toe to root cracking (above the curve, the failure mode is root cracking, and below the curve, the failure mode is toe cracking) (Fig. 30). Furthermore, some points from the experimental test in the literature (indicated as Hui and Vilhauer) and our experimental tests are shown. As can be seen, below the line the failure mode is toe cracking. One point above the line has toe cracking. Toe failure may be because of inappropriate HFMI treatment. Hui et al. [18] mentioned in their paper that in one case, the HFMI treatment was not performed correctly. It could also be the case that the weld residual stress at the root is compressive, and of course, there is a degree of weld penetration that is not modelled in the ENS models which will give lower stress concentration at the root side. The failure mode in our analysis was from root to the weld surface. In the region near the line, both root cracking and root cracking are observed. We suspect that the points marked as "run out" would result in root cracking if the fatigue tests were continued.

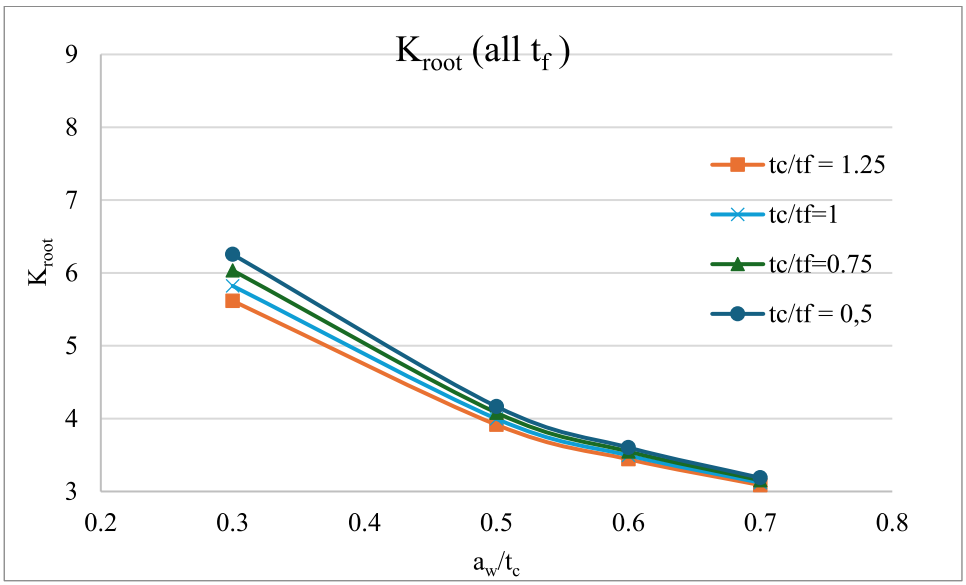

Fig. 27 The K_{root} versus the weld size to cover plate thickness ratio for all t_f

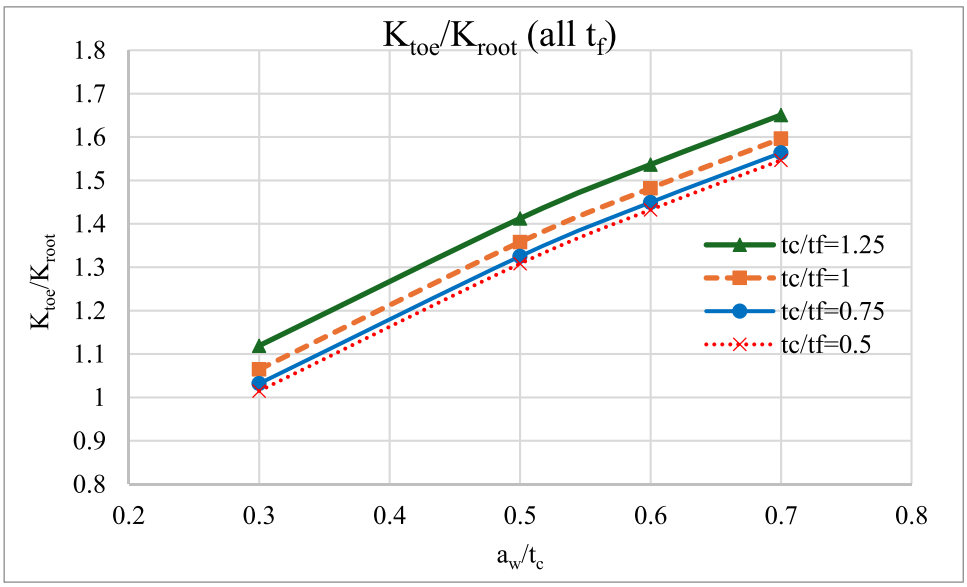

Fig. 28 The ratio of K_{toe} to K_{root} versus the weld throat size to cover plate thickness ratio

6 Conclusion

In this study, FE modelling was used to investigate how cover plate thickness, flange thickness, and weld throat size impact the fatigue life of welded cover plates, when the ends of these plates are treated with high-frequency mechanical impact (HFMI) treatment. Furthermore, the effect of the presence of shear stress and loading conditions on the stresses at the weld toe and root were investigated. Based on more than 120 cases analyzed using the effective notch stress method, expressions for estimating stress concentration factors at the weld toe and root for pure bending conditions were derived. These expressions can be used in the design of HFMI-treated cover plates to estimate the fatigue life of these details with reference to different failure modes. The key findings are as follows:

- The weld throat size is the factor that most significantly affects the stress concentration factors both at weld toe and root. A reduction in the weld throat size leads to an increase in both K_{toe} and K_{root} and a decrease in K_{toe}/K_{root}, indicating higher risk for root cracking.
- The stress concentration factor at the toe also depends on t_c/t_f especially when smaller weld throat sizes are selected.
- When the welded cover plate is subjected to loading at low-stress levels, HFMI treatment has little to no effect on the fatigue life of welded cover plates. The failure mode for low-stress loading is root cracking.

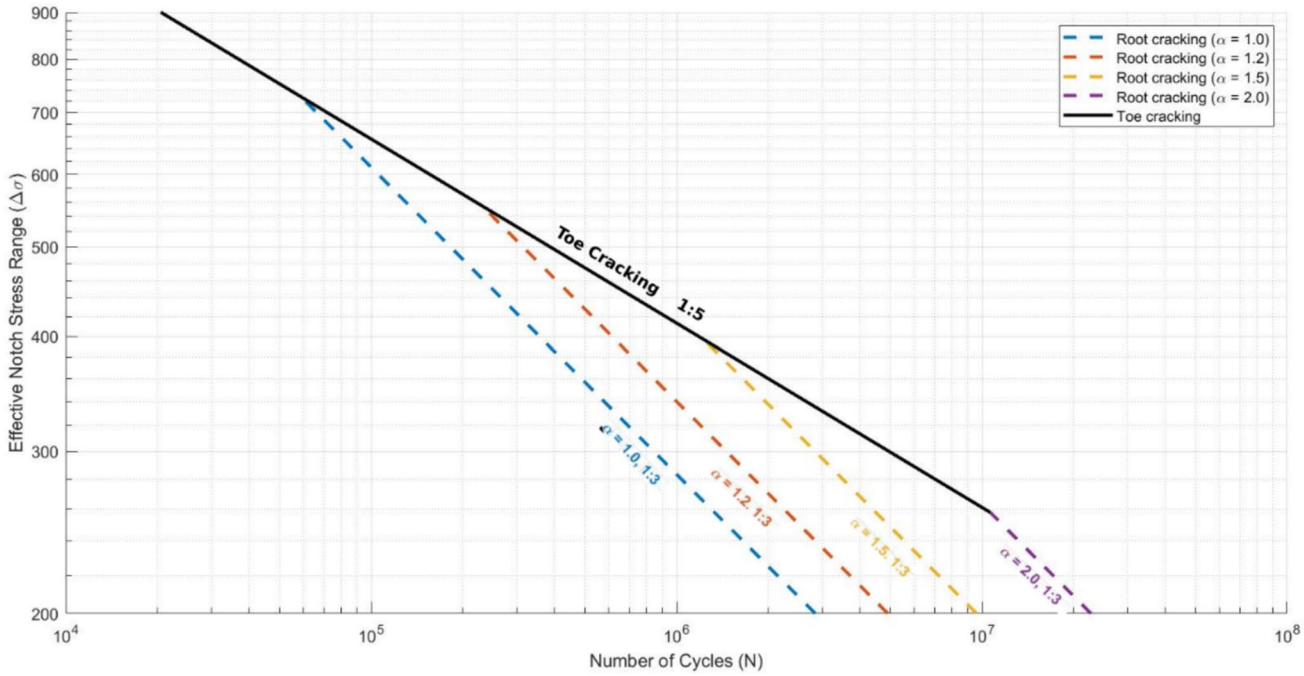

Fig. 29 S–N curves for HFMI-treated for different values of $\alpha(K_{toe}/K_{root})$

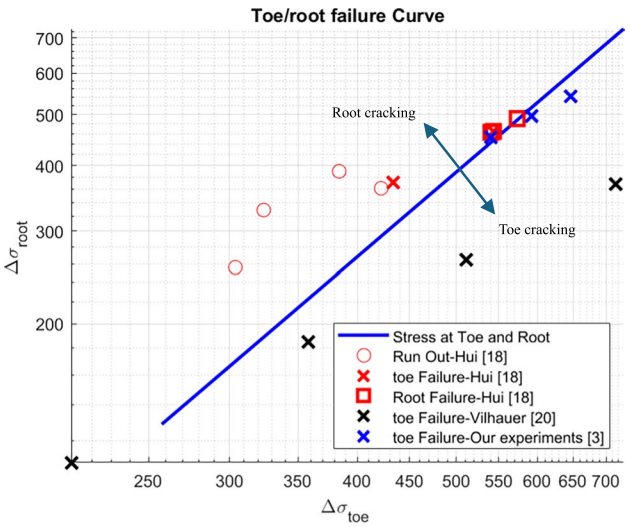

Fig. 30 Curve for failure mode on logarithmic scale

- HFMI-treated cover plates should be checked for both toe and root cracking. The risk of root cracking depends on the geometrical parameters, the material, and the stress range.
- Connections can be designed, either to avoid root cracking by selecting plate thicknesses and weld sizes that mitigate this failure mode, or by verifying both toe and root failure.
- If possible, a_w/t_c should be greater than 0.5. When it exceeds 0.5, the stress concentration factor at the root becomes lower, and the risk of root failure decreases. Furthermore, the dependency of stress concentration factors at the toe and root to thickness ratio becomes negligible for a_w/t_c greater than 0.5 (as shown in Figs. 24, 25, and 26).

Acknowledgements The work presented in this paper is part of an ongoing research project on the fatigue strength of HFMI-treated welded cover plates. The authors acknowledge the funding provided by the Swedish Transport Administration (Trafikverket). The support and contribution of Jens Häggström are also appreciated.

Author contribution M. Al-Emrani conceived of the presented idea. M. Noghabi worked out the technical details and performed the numerical calculations (FEM). M. Al-Emrani carried out the experiments. All authors discussed the results and contributed to the final manuscript.

Funding Open access funding provided by Chalmers University of Technology. The work presented in this paper is part of an ongoing research project on the fatigue strength ofHFMI-treated welded cover plates. The authors acknowledge the funding provided by the SwedishTransport Administration (Trafi kverket).

Data availability The data that supports the findings of this study are available from the corresponding author upon reasonable request.

Declarations

Competing interests The authors declare no competing interests.

References

1. Fisher JW, Hausammann H, Sullivan MD, and Pense A.W (1979) Detection and repair of fatigue damage in welded highway bridges. in National cooperative highway research program Report, no. 206. Washington, DC: Transportation Research Board.
2. Hu J (2011) A study on cover plate design and monopole strengthening application. Thin-Walled Struct 49(9):1098–1107. https://doi.org/10.1016/j.tws.2011.04.002
3. Al-Emrani M, Hedegård J, and Pétursson H (2024) "Fatigue life improvement of welded cover-plates using high frequency mechanical impact treatment," presented at the IABSE Congress, San José 2024: beyond structural engineering in a changing world, San José, Costa Rica, pp. 580–586. https://doi.org/10.2749/sanjose.2024.0580.
4. American Association of State Highway and Transportation Officials (2012) *AASHTO LRFD bridge design specifications, customary U.S. units*. Washington, DC: American Association of State Highway and Transportation Officials. Accessed: Nov. 05, 2015. [Online]. Available: http://app.knovel.com/hotlink/toc/id:kpAASHTO32/aashto-lrfd-bridge
5. EN 1993 (2005) Eurocode 3: Design of steel structures - Part 1–9: fatigue. Brussels: European Committee for Standardization (CEN).
6. Yıldırım HC (2017) Recent results on fatigue strength improvement of high-strength steel welded joints. Int J Fatigue 101:408–420. https://doi.org/10.1016/j.ijfatigue.2016.10.026
7. Harati E, Svensson L-E, Karlsson L, Hurtig K (2016) Effect of HFMI treatment procedure on weld toe geometry and fatigue properties of high strength steel welds. Procedia Struct Integr 2:3483–3490. https://doi.org/10.1016/j.prostr.2016.06.434
8. Edgren M, Barsoum Z, Åkerlind K, Al-Emrani M (2019) Evaluation of HFMI as a life extension technique for welded bridge details. Procedia Struct Integr 19:73–80. https://doi.org/10.1016/j.prostr.2019.12.009
9. Al-Karawi H, Al-Emrani M (2021) The efficiency of HFMI treatment and TIG remelting for extending the fatigue life of existing welded structures. Steel Constr 14(2):95–106. https://doi.org/10.1002/stco.202000053
10. Marquis GB, Barsoum Z (2016) IIW Recommendations for the HFMI treatment. IIW Collection Singapore: Springer Singapore. https://doi.org/10.1007/978-981-10-2504-4
11. Leitner M, Barsoum Z, Schäfers F (2016) Crack propagation analysis and rehabilitation by HFMI of pre-fatigued welded structures. Weld World. https://doi.org/10.1007/s40194-016-0316-x
12. Fuštar B, Lukačević I, Skejić D, Garašić I (2024) Fatigue tests of S690 as-welded and HFMI-treated details with longitudinal and transverse attachments. Results Eng 23:102386. https://doi.org/10.1016/j.rineng.2024.102386
13. Marquis GB, Mikkola E, Yildirim HC, Barsoum Z (2013) Fatigue strength improvement of steel structures by high-frequency mechanical impact: proposed fatigue assessment guidelines. Weld World 57(6):803–822. https://doi.org/10.1007/s40194-013-0075-x
14. Lihavainen V-M, Marquis G, Statnikov ES (2004) Fatigue strength of a longitudinal attachment improved by ultrasonic impact treatment. Weld World 48(5–6):67–73
15. Fueki R, Takahashi K (2018) Prediction of fatigue limit improvement in needle peened welded joints containing crack-like defects. Int J Struct Integr 9(1):50–64. https://doi.org/10.1108/IJSI-03-2017-0019
16. Al-Karawi H, Von Bock Und Polach RUF, Al-Emrani M (2021) Fatigue life extension of existing welded structures via high frequency mechanical impact (HFMI) treatment. Eng Struct 239:112234. https://doi.org/10.1016/j.engstruct.2021.112234
17. Roy S, Fisher JW (2006) Modified AASHTO design S – N curves for post-weld treated welded details. Bridge Struct 2(4):207–222. https://doi.org/10.1080/15732480601103630
18. Hui JF, Lloyd JB, Connor RJ (May2018) Fatigue life improvement of welded girders with ultrasonic impact treatment. Purdue University. https://doi.org/10.5703/1288284316654
19. Leitner M, Stoschka M (2020) Effect of load stress ratio on nominal and effective notch fatigue strength assessment of HFMI-treated high-strength steel cover plates. Int J Fatigue 139:105784. https://doi.org/10.1016/j.ijfatigue.2020.105784
20. Vilhauer B, Bennett CR, Matamoros AB, Rolfe ST (2012) Fatigue behavior of welded coverplates treated with ultrasonic impact treatment and bolting. Eng Struct 34:163–172. https://doi.org/10.1016/j.engstruct.2011.09.009
21. Dai P et al (2023) Numerical study on local residual stresses induced by high frequency mechanical impact post-weld treatment using the optimized displacement-controlled simulation method. J Manuf Process 92:262–271. https://doi.org/10.1016/j.jmapro.2023.03.002
22. Baumgartner J, Bruder T (2013) An efficient meshing approach for the calculation of notch stresses. Weld World 57(1):137–145. https://doi.org/10.1007/s40194-012-0005-3
23. Ahola A, Skriko T, Lipiäinen K, Björk T (2021) On the weld root fatigue strength and improvement techniques for non-load-carrying transverse attachment joints with single-sided fillet welds and made of mild and ultra-high-strength steels. Eng Struct 249:113373. https://doi.org/10.1016/j.engstruct.2021.113373
24. *Matlab 2013b*. (2013). The MathWorks, Inc., Natick, Massachusetts, United States. [Online]. Available: https://se.mathworks.com/
25. Al-Karawi H, Shams-Hakimi P, Pétursson H, Al-Emrani M (2024) Mean stress effect in high-frequency mechanical impact (HFMI)-treated welded steel railway bridges. Steel Constr 17(2):81–92. https://doi.org/10.1002/stco.202200046
26. Al-Karawi H, Shams-Hakimi P, Al-Emrani M (2022) Mean stress effect in high-frequency mechanical impact (HFMI)-treated steel road bridges. Buildings 12(5):545. https://doi.org/10.3390/buildings12050545